

Plant WEE1 Kinase Interacts with a 14-3-3 Protein, GF14 ω but a Mutation of WEE1 at S485 Alters Their Spatial Interaction

Anne Lentz Grønlund^{1,2,3}, J. Richard Dickinson¹, Peter Kille¹, John L. Harwood¹, Robert J. Herbert², Dennis Francis^{1,*} and Hilary J. Rogers¹

¹School of Biosciences, Cardiff University, Park Place, Cardiff. CF10 3TL, UK

²Institute of Science and the Environment, University of Worcester, Henwick Grove, Worcester, WR2 6AJ UK

³Rothamsted Research, Harpenden AL5 2JQ, UK

Abstract: In animals, 14-3-3 proteins bind two cell cycle proteins WEE1 and CDC25 stabilising their phosphorylated state. We report here for the first time interactions between WEE1 and 14-3-3 proteins both *in vitro* and *in vivo* in plants. The *Arabidopsis* 14-3-3 family partitions into either an Epsilon or Non-Epsilon group. In a yeast 2-hybrid screen *Arabidopsis* WEE1 interacted with the Non-Epsilon group. Subsequently, we focussed on Non-Epsilon GF14 ω , a 14-3-3 expressed more strongly in proliferative than in non-proliferative cells and which is able to rescue a cell cycle checkpoint mutant in yeast. The WEE1/GF14 ω interaction was confirmed by an *in vitro* co-immunoprecipitation assay and *in vivo* in tobacco BY-2 cells by bi-molecular fluorescence complementation. Sub-cellular interaction between WEE1 and GF14 ω occurs in the nucleus of interphase cells. Additionally an interaction was very occasionally observed in the cross wall between cells. Their small stature and independent observations of callose, of the type that typically forms in new cell plates, suggests that this additional interaction might be occurring at cytokinesis. An S485A mutation of WEE1 abolished this interaction *in vitro* and altered the spatial interaction *in vivo* indicating that this is a likely regulatory phosphorylation target for the WEE1/GF14 ω interaction.

Key Words: 14-3-3 Proteins, *Arabidopsis thaliana*, bi-molecular fluorescence complementation cell cycle, WEE1.

INTRODUCTION

In eukaryotes the cell cycle is regulated by cyclin dependent kinases (CDKs) at G1/S and G2/M [1] in a mechanism conserved from yeast to animals [2]. CDKs are tightly regulated by their association with cyclins through phosphoregulation. At the G2/M transition, CDKs are also phosphoregulated positively by CDC25 phosphatase [3], and negatively by WEE1 kinase, which has been identified in yeasts [4], animals [5] and plants [6-8]. In normal animal cell cycles, WEE1 is located in the nucleus during interphase but is partitioned away from chromosomes from late prophase to early telophase [9]. Nuclear WEE1 kinase activity is high during interphase but absent during mitosis [5] whilst CDK1-cyclinB1 is located in the cytoplasm in interphase and in the nucleus at G2/M [1]. Thus spatial and molecular controls prevent unscheduled mitosis occurring in interphase and entrain the CDK to be active at the G2/M transition in mitotically competent cells. However, we know very little about spatial control of the plant cell cycle.

The Ataxia-telangiectasia mutated/related (ATM/ATR) proteins and in *S. pombe* the RAD3 protein are induced if DNA replication is perturbed or DNA is damaged [10-12].

They trigger a pathway of DNA dependent kinases that repair the DNA defect and phosphorylate and activate the checkpoint kinases, CHK1 and/or CHK2. These kinases participate in the stabilisation of WEE1 kinase activity ensuring that the phosphorylation of the CDK/cyclin complex is maintained and that the cell is arrested in G2 [13]. CHK1/2 also phosphorylates and inactivates CDC25 phosphatase to keep the CDC2/CyclinB complex inactive. When DNA replication is normalised or DNA damage is repaired CDC25 is dephosphorylated and restores the activity of the CDK/cyclin complex [14, 15].

In yeast and animal checkpoints, the phosphorylations of WEE1 and CDC25 are at least partly stabilised by the binding of 14-3-3 proteins [16-21]. These proteins have an important role in cell cycle checkpoints because they bind and protect phosphorylated sites on both WEE1 and CDC25, thereby maintaining their activation or inactivation, respectively [20, 22, 23]. 14-3-3 proteins bind their target proteins *via* high affinity phosphorylation-dependent binding motifs: RSXpSXP (mode I) and RXXXpSXP (mode II) [24, 25]. Seven 14-3-3s have been identified in humans and 13 in *Arabidopsis* [26]. Although the overall amino acid sequence of 14-3-3 proteins is highly conserved [27], the *Arabidopsis* 14-3-3s are divided into two groups, Epsilon and Non-Epsilon, based on their amino acid sequence [26]. 14-3-3 proteins are expressed in a wide range of tissues and cell types but so far only two reports suggest that plant 14-3-3s are involved in plant cell cycle regulation [28, 29].

*Address correspondence to this author at the School of Biosciences, Cardiff University, Park Place, Cardiff. CF10 3TL, UK; Tel: + 44-29-2087-5086; Fax: +44- 29- 2087- 4305; E-mail: francisd@cardiff.ac.uk

In *Arabidopsis*, *wee1* T-DNA insertion lines are hypersensitive to hydroxyurea and zeocin, agents that induce the DNA replication and DNA damage checkpoints, respectively, supporting a role for *WEE1* in these checkpoint mechanisms [30]. Although over-expression of *WEE1* results in a G2/M block, in non-stressed conditions the T-DNA insertion lines seem to develop normally raising doubts about a regulatory role for *Arath*; *WEE1* in a normal plant cell cycle [30]. This contrasts with other eukaryotes in which *WEE1* is an essential gene [1, 2, 4]. This divergent role for plant *WEE1* led us to ask whether its regulation through protein-protein interaction is also different in plants.

The aim of the work presented here was thus to test the hypothesis that *Arabidopsis* *WEE1* interacts with 14-3-3 proteins and to localise this interaction within plant cells. We demonstrated an interaction between *Arath*; *WEE1* and GF14 ω both *in vitro* and *in vivo* and identified both the location of the interaction *in vivo* and a likely phosphoregulatory target for this interaction.

MATERIALS AND METHODS

Constructs and Y2H Screens

For the bait plasmid, the coding sequence of *Arath*; *WEE1* was amplified using primers *Arath*; *WEE1* FW 5'-CAT-GGAGAATTCATGTTTCGAGAAGAACG-3' and *Arath*; *WEE1* RV 5'-ACGTTTCGACCTCAACCTCGAATCCTATC-3' and fused in-frame with the GAL4 DNA-binding domain in the pBD-GAL4-Cam vector using *EcoRI* and *Sall* sites. For the target plasmids, the coding sequences of GF14 ω , λ , κ , χ , ϕ , ψ , ν and υ were amplified using primers *Arath*; GF14 ω FW 5'-CGGGATCCATGGCGTCTGGGCGTGAA-3' and *Arath*; GF14 ω RV 5'-CGGAATCCTCAGGCCTCATCCATCTGCT-3'; *Arath*; GF14 λ FW 5'-CGGGATCCATGGCGGCGACATTAGGCA-3' and *Arath*; GF14 λ RV 5'-CGGAATCCTCAGGCCTCATCCATCTGCT-3'; *Arath*; GF14 κ FW 5'-CGGGATCCATGGCGGCGACCTTAAGCA-3' and *Arath*; GF14 κ RV 5'-CGGAATCCTCAGGCCTCATCCATCTGCT-3'; *Arath*; GF14 ψ FW 5'-AAGGATCCATGTCGACAAGGGAAGA-GAATG-3' and *Arath*; GF14 ψ RV 5'-AATTGCTAGCTTACTCGGCACCATCGGGCT-3'; *Arath*; GF14 ν FW 5'-AAGGATCCATGTCGTCTTCTCGGGAAGAG-3' and *Arath*; GF14 ν RV 5'-AATTGCTAGCTCACTGCCCTGTCTCAGCTG-3'; *Arath*; GF14 υ FW 5'-AAGGATCCATGTCCTCTGATTCGTCCCGG-3' and *Arath*; GF14 υ RV 5'-AATTGCTAGCTCACTGCGAAGGTGGTGGTT-3'; *Arath*; GF14 ϕ FW 5'-AAGGATCCATGGCGGCACCAC-CAGCAT-3' and *Arath*; GF14 ϕ RV 5'-AATTGCTAGCTT-AGATCTCCTTCTGTTCTTCTCAG-3'; *Arath*; GF14 χ FW 5'-AAGGATCCATGGCGACACCAGGAGCTTC-3' and *Arath*; GF14 χ RV 5'-AATTGCTAGCCTAGGATTGTTGC-TCGTCAGC-3'. The coding sequences were fused in-frame with the GAL4 DNA-binding domain of the pAD-GAL4-2.1 vector using *BamHI* and *NheI* sites. The insertion of the coding sequences into the Y2H vectors was confirmed by sequencing.

Both bait and target vector were transformed into the budding yeast strain YPH499 (*MATa ura3-52 lys2-801 ade2-101 trp1 Δ 63-901 his3 Δ 200 leu2 Δ 1, gal4-542 gal80-538 LYS2::UAS GAL1-TATAGAL1-HIS3 URA3::UAS GAL4 17mers(x3)-TATACYC1-lacZ* (Stratagene) and plated

onto trp-leu- minimal medium containing 40 mM 3-amino-1, 2, 4-triazole (3-AT; Sigma). Plates were incubated at 30°C and colonies were re-patched onto his⁻ minimal medium. His⁺ patches were assayed for β -galactosidase activity using a filter lift assay (Stratagene).

ONPG Assay

The assay was performed by inoculating transformed YRG2 cells into 5 mL SGR medium (1.67 g/L Difco Yeast Nitrogen Base (w/o amino acids), 5 g/L ammonium sulphate, 20 g/L galactose, 10 g/L raffinose \pm 20 g/L Difco bacto agar) and cultures were incubated in a Gallenkamp orbital incubator at 160 rpm at 30°C until an OD₆₀₀ 0.6 – 0.8. Cells were harvested by centrifugation in an MSE Centaur 2 centrifuge for 10 min at 4000 rpm and the pellet was resuspended in 5 mL of Z-buffer (10.7 g/L Na₂HPO₄·2H₂O, 6.2 g/L NaH₂PO₄·2H₂O, 0.75 g/L KCl, 0.246 g/L MgSO₄·7H₂O) and placed on ice. OD₆₀₀ was measured and to each sample was added one drop of 0.1% SDS and two drops of chloroform. Tubes were vortexed for 15 sec and incubated at 30°C for 15 min and 160 μ L of 4 mg/mL ONPG (Sigma) were added. Tubes were vortexed well for 10 s and incubated at 30°C for 20 min. After 20 min samples were removed and 400 μ L of 1 M sodium carbonate were added. Samples were spun down and OD₄₂₀ and OD₅₅₀ of the supernatant were measured. Miller units were calculated as follows: $U = 1000 \times [(OD_{420}) - (1.75 \times OD_{550})] / [(time) \times (volume) \times OD_{600}]$, where time is the incubation time with ONPG (min) and the volume is the volume of initial culture used (mL).

Constructs and Co-Immunoprecipitation

Constructs were made using the pESC-TRP yeast epitope tagging vector (Stratagene) carrying coding sequences: *Arath*; GF14 ω only, *Arath*; *WEE1* only, *Arath*; GF14 ω /*Arath*; *WEE1*. The coding sequence of *Arath*; GF14 ω was PCR-amplified using primers FW: 5'-ATGGGGATCCCAATGGCGTCTGGGCGTGAAG-3' and RV: 5'-GGATCCTCAC-TGCTGTTCTCCTCGG-3' and inserted into the *BglIII* site of the pESC-TRP vector to introduce a FLAG epitope tag at the N-terminus. The coding sequence of *Arath*; *WEE1* was PCR amplified using primers FW: 5'-ATCGGGATCCATGTT-CGAGAAGAACGGAA-3' and RV: 5'-GCTAGTCGACCACTCGAATCCTATCAAAC-3' and inserted in the pESC-TRP vector using the *BamHI* and *Sall* sites to introduce a c-myc epitope tag at the C-terminus. Insertions of *Arath*; *WEE1* and *Arath*; GF14 ω into vectors were confirmed by sequencing.

The constructs were transformed into the budding yeast strain YPH499 (*ura3-52 lys2-801 ade-101 ochre trp1- Δ 63 his3- Δ 200 leu2- Δ 1*). Proteins were extracted from the yeast cells by vortexing with glass beads in lysis buffer (50 mM Hepes (pH 7.5), 100 mM NaCl, 10% glycerol, 60 mM β -glycerophosphate, 1 mM sodium vanadate, 0.5 mM phenylmethylsulfonyl fluoride (PMSF), complete protease inhibitors: 1 tablet/10 ml (Roche)). Protein extracts (~1 mg) were bound to 40 μ L Anti-FLAG M2 affinity gel (Sigma) in a volume of 1 ml by rotation at 4°C over night. The affinity gel was subsequently washed three times with TBS and bound proteins were eluted by adding 0.1 M glycine pH. 3.5 to the affinity gel. Eluates were mixed with 2x SDS sample buffer [1%SDS, 45 mM Tris-HCl (pH 6.8), 50 mM DTT, 10% glycerol, 0.1 mg ml⁻¹ bromophenol blue] and separated by

SDS-PAGE and western-blotted. Duplicate blots were probed with FLAG (1:8,000 primary antibody dilution) and c-myc (1:100 primary antibody dilution) monoclonal antibodies (Sigma) or WEE1 (1:1000 primary antibody dilution) polyclonal antibody (Sigma-Genosys).

The WEE1 antibody was raised in rabbit using the peptide DADAADGDNKDFILC located at amino acid position 87 in the N-terminal regulatory domain of tobacco (*Nicotiana tabacum*) WEE1, Nicta;WEE1. The peptide was synthesized chemically and checked to >50% purity. It was conjugated to keyhole limpet haemocyanin carrier using equal amounts (w/w, 2-3 mg) of carrier and peptide for use as an antigen. Antigens were injected into the rabbits in 100-200 µg amounts, subcutaneously in rabbits at 2-week intervals over a 70 day period, and the appearance of antibodies was determined by ELISA. The antibody specificity was tested against Nicta;WEE1 and Arath;WEE1 expressed in *E. coli* and against total protein from tobacco BY2 cells and Arabidopsis seedlings. The antibody identified a band of the correct molecular weight for WEE1 from both tobacco and Arabidopsis (data not shown). Proteins were visualised using ECL western blotting reagents (Amersham Biosciences).

Constructs, Stable Transformation of Tobacco BY-2 Cell Cultures and BiFC

BiFC vectors were kindly donated by Dr. J. Kudla, Münster University, Germany. For constructing the pSPYNE 35S vectors, the coding sequences of *Arath;WEE1* and *Arath;GF14ω* were PCR amplified using primers WEE1 FW: 5'-ATACTAGTATGTTTCGAGAAGAACGGAAG-3' and RV: 5'-TAGGTACCACCTCGAATCCTATCAAACA-3'; *GF14ω* FW: 5'-ATACTAGTATGGCGTCTGGGCGTGAAGA-3' and RV: 5'-TAGGTACCCTGCTGTTCCCTGGTCG-3'. The coding sequences were fused in-frame to the N-terminal part of the YFP using *SpeI* and *KpnI* sites. For constructing the pSPYCE 35S vectors, the coding sequences of *Arath;WEE1* and *Arath;GF14ω* were PCR amplified using primers WEE1 FW: 5'-ATACTAGTATGTTTCGAGAAGAACGGAAG-3' and RV: 5'-TACTCGAGACCTCGAATCCTATCAAACA-3'; *GF14ω* FW: 5'-ATACTAGTATGGCGTCTGGGCGTGAAGA-3' and RV: 5'-TACTCGAGCTGCTGTTCCCTCGGTTCG-3'. The coding sequences were fused in-frame to the C-terminal part of the YFP using *SpeI* and *XhoI* sites. The insertions of *Arath;WEE1* and *Arath;GF14ω* into the respective vectors were confirmed by sequencing.

Stable transformation of tobacco BY-2 cells was achieved by the method of An [43] modified with the addition of 20 µM acetosyringon (Sigma-Aldrich) during co-cultivation of the tobacco BY-2 cells with the *Agrobacterium* (LBA4404) carrying the pSPYNE 35S constructs. Transformants were selected on solidified BY2 medium (0.8% agar) supplemented with 250 µg/ml Timentin and 80 µg/ml hygromycin. Calli were cultured in 50 ml BY-2 medium, 250 µg/ml Timentin and 80 µg/ml hygromycin until stationary phase (1 – 3 weeks).

For the BiFC experiments, the stable pSPYNE 35S lines were transiently transformed with the pSPYCE 35S constructs in *Agrobacterium* (EHA105). Ten ml aliquots of LB medium were inoculated with a single colony of freshly

streaked *Agrobacterium* (EHA105) carrying the pSPYCE 35S vectors. Cultures were incubated overnight in a Gallenkamp orbital incubator at 160 rpm at 30°C. Three day-old sub-cultures of the stable tobacco BY-2 pSPYNE 35S cell lines were used for the transient transformations (prior to the transient transformation, the stable tobacco BY-2 cell lines were sub-cultured without hygromycin at least twice). To 7 ml of the stable tobacco BY-2 pSPYNE 35S cell culture, 200 µM acetosyringon was added. The acetosyringon-treated cells were then co-cultivated with 200 µl of the overnight *Agrobacterium* (EHA105) carrying the pSPYCE 35S constructs in Petri dishes containing BY-2 agar without selection. Plates were wrapped in Nesco film and incubated in darkness for 72 h at 28°C. Yellow fluorescence was assessed using a fluorescence microscope (Olympus BH2) equipped with a 530 nm filter using exactly the same parameters for all the images captured (adjusted with the auto level function and colour replacement function in Adobe Photoshop®).

The positive control for the BiFC experiments was a stable pSPYNE 35S *Arath;bZIP63* tobacco BY-2 line transiently transformed with pSPYCE 35S *Arath;bZIP63* [31]. The negative control was a stable pSPYNE 35S *Arath;bZIP63* tobacco BY-2 line transiently transformed with pSPYCE 35S *Arath;WEE1*. For the detection of callose on cell cross-walls, 20 µl of BY-2 cells was mixed with 0.01% (w/v) aniline blue (Gurr-BDH, UK) in a 3% (w/v) solution of ANALAR sucrose (BDH, UK). Slides were left for 1 h before being examined using fluorescence microscopy (as detailed above).

Site-Directed Mutagenesis

Site-directed mutagenesis of *Arath;WEE1* was performed using the QuickChange® Site-directed Mutagenesis kit (Stratagene) with primers FW: 5'-GTCGGCCTGCTGCTAGAGAATTACTGGAC-3' and RV: 5'-CTAGCAGCAGGCCGACGCTTCGGATC-3'. The PCR program was: 1 cycle of initial denaturation (30 s at 95°C); 16 cycles of denaturation (30 s at 95°C; annealing (1 min at 55°C); extension (20 min at 68°C); 1 cycle of final extension (1 h at 68°C). PCR reactions were digested with 10 U *DpnI* for 1 h at 37°C and EtOH precipitated. The precipitated DNA was transformed into *E. coli* DH5α cells and the S485A mutation was verified by sequencing of the original mutagenised plasmid. The *Arath;WEE1* (S485A) coding sequence was re-cloned into an empty pBD-Gal4-cam vector via *Sall/EcoRI* restriction sites and into the empty pSPYCE 35S vector with *SpeI/XhoI* restriction sites as previously described.

RESULTS

Arath; WEE1 Interacts with the Non-Epsilon Group of 14-3-3s

Previous work established that some of the Non-Epsilon 14-3-3 proteins could rescue cell cycle defects in fission yeast mutants [28]. Hence, a targeted yeast two hybrid (Y2H) screen tested whether *Arath;WEE1* interacted with the Non-Epsilon group of 14-3-3 proteins comprising: GF14κ (kappa), GF14λ (lambda), GF14ν (nu), GF14υ (upsilon), GF14φ (phi), GF14χ (chi), GF14ψ (psi) and GF14ω (omega). Bait and target plasmids were co-transformed into yeast and transformants were detected if they grew on me-

dium deficient in tryptophan and leucine. Transformants carrying the *Arath*;WEE1 bait plasmid co-transformed with the Non-Epsilon 14-3-3 target plasmids grew on medium lacking histidine indicating transcriptional activation of the *HIS3* reporter gene by an interaction between *Arath*;WEE1 and all of the Non-Epsilon 14-3-3 proteins (data not shown). In a second screen, the interaction was verified when the transformants carrying the *Arath*;WEE1 bait plasmid, co-transformed with the Non-Epsilon 14-3-3 target plasmids, activated transcription of the *LacZ* reporter gene in a non-quantitative assay (blue colouration of the yeast in the filter lift assay, Fig. 1).

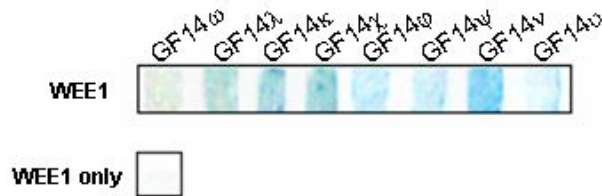


Fig. (1). *Arath*; WEE1 interacts with Non Epsilon 14-3-3 proteins *in vitro*. Qualitative filter lift assay of yeast colonies co-expressing *Arath*;WEE1 and 14-3-3 proteins belonging to the Non-Epsilon group as a control, yeast transformed with the *Arath*;WEE1 bait plasmid only was used showing that the *Arath*;WEE1 bait is not capable of auto-activating the *LacZ* reporter gene.

Interaction Between *Arath*;WEE1 and *Arath*;GF14 ω Verified by Co-Immunoprecipitation

Of three interacting Non-Epsilon 14-3-3 proteins, GF14 κ , λ and ω , only the latter was expressed more strongly in proliferative regions but less so in non-proliferative regions [29]. Hence, we focussed on the WEE1/GF14 ω interaction which was confirmed *in vitro* by co-immunoprecipitation using the pESC yeast epitope-tagging vector system (Stratagene). *Arath*;WEE1 was tagged with c-myc, while *Arath*;GF14 ω was FLAG tagged. Proteins were pulled down with the anti-FLAG antibody, and Western blots probed with FLAG and c-myc antibodies (Fig. 2A) revealed a band of 56 kDa corresponding to the size of *Arath*;WEE1 in the *Arath*;WEE1 c-myc/*Arath*;GF14 ω FLAG eluate, indicating that *Arath*;WEE1 binds to *Arath*;GF14 ω . The 56 kDa band corresponding to the size of *Arath*;WEE1 was not detectable in the control co-immunoprecipitations (*Arath*;GF14 ω FLAG only or *Arath*;

WEE1 c-myc only) and, a band of 29 kDa corresponding to the size of *Arath*;GF14 ω was detected in all co-immunoprecipitation eluates except in the *Arath*;WEE1 c-myc control (Fig. 2A). Additionally, *Arath*;GF14 ω could bind to native *Arath*;WEE1. A total protein extract from *Arabidopsis* seedlings was mixed with protein extracted from the *Arath*;GF14 ω FLAG-producing yeast and when proteins were pulled down with anti FLAG antibody and Western blots were probed with an antibody raised against plant WEE1, a band of 56 kDa corresponding to the size of *Arath*;WEE1 could be detected (Fig. 2B).

In Vivo Interaction Between *Arath*;WEE1 and *Arath*;GF14 ω Shown by Bi-molecular Fluorescence Complementation (BiFC)

The BiFC technique can analyze protein-protein interactions in a wide-range of plant tissues and cell types. So far it has been used in foliage by leaf infiltration techniques or in plant cell-derived protoplasts by transient transformation [32, 33]. To our knowledge, this is the first report of a functional BiFC system in plant cell suspension culture. This has the advantage over the use of protoplasts in providing sub-cellular localization and, unlike the use of leaf infiltrations, does not require confocal microscopy. Analyses were performed by *Agrobacterium*-mediated transient transformation of stable tobacco BY-2 lines carrying one of the two split-YFP constructs in the pSPYNE vector. pSPYNE 35S *Arath*;bZIP63 and pSPYCE 35S *Arath*;bZIP63 were the positive controls and in BY2 interphase cells, yellow fluorescence was detected in the nucleus (Fig. 3A), in agreement with the use of these vectors in protoplasts (Walter *et al.*, 2004). A stable tobacco BY-2 cell culture carrying pSPYNE 35S *Arath*;bZIP63 transformed transiently with pSPYCE 35S *Arath*;WEE1 was used as the negative control and fluorescence could not be observed (Fig. 3B). Since 14-3-3 proteins can form dimers [34-36], a stable BY-2 cell line carrying the pSPYNE 35S *Arath*;GF14 ω was transiently transformed with pSPYCE 35S *Arath*;GF14 ω . In contrast to the *Arath*:bZIP63, fluorescence was seen mainly in the nucleus but also in the wall between adjacent cells (Fig. 3C).

When a tobacco BY-2 cell culture carrying pSPYNE 35S *Arath*;GF14 ω was transiently transformed with pSPYCE 35S *Arath*;WEE1, yellow fluorescence was detected in

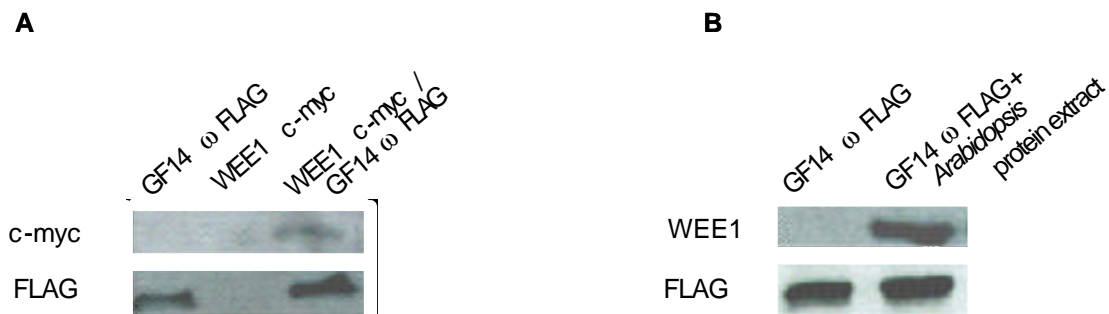


Fig. (2). Biochemical confirmation of the interaction *in vitro*. Co-immunoprecipitation analysis of *Arath*;WEE1 and *Arath*;GF14 ω (A) FLAG and c-myc antibody-probed western blots of FLAG immunoprecipitated proteins extracted from yeast transformants carrying pESC constructs: *Arath*;GF14 ω FLAG only, *Arath*;WEE1 c-myc only, *Arath*;WEE1 c-myc/ GF14 ω FLAG. (B) FLAG and WEE1 antibody-probed western blots of FLAG immunoprecipitated proteins extracted from yeast transformants carrying pESC constructs: *Arath*;GF14 ω FLAG only and *Arath*;GF14 ω FLAG mixed with 1 mg of *Arabidopsis* protein extract.

interphase cells in the nucleus (Fig. 4A) and in the periphery of the cytoplasm (Fig. 4B). However, yellow fluorescence was also prominent in the cell wall between shorter cells (Fig. 4C). We hypothesise that this latter signal is associated with the cell plate at cytokinesis. To test this, we used aniline blue as a marker of cytokinesis (Fig. 5); it stains callose

at the newly forming cell plate [37]. There was a very low frequency (0.03%) of such stained cross walls in comparable cells used for BiFC. Thus the very low frequency of both BiFC positive signal on cross walls between small cells (Fig. 4C) and stained cross walls by aniline blue, suggests an interaction between WEE1 and GF14 ω at cytokinesis.

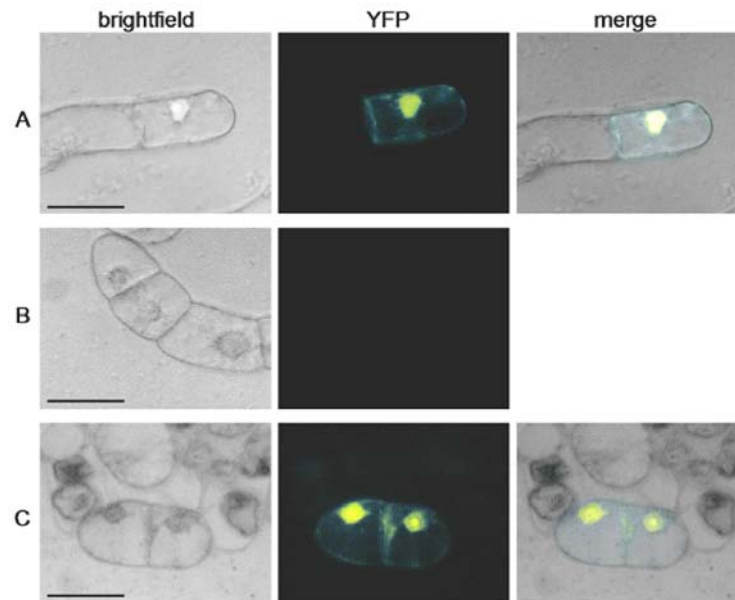


Fig. (3). Confirmation of SPYCE/SPYNE interaction *in vivo*. BiFC analysis of (A) the *Arath*;bZIP63/*Arath*;bZIP63 homodimerization (positive control), transient *Agrobacterium*-mediated transformation of the pSPYNE 35S *Arath*;bZIP63 BY-2 cell line with pSPYCE 35S *Arath*;bZIP63. Yellow fluorescence could be detected only in the nucleus. (B) *Arath*;bZIP63/*Arath*;WEE1 (negative control), transient *Agrobacterium*-mediated transformation of the pSPYNE 35S *Arath*;bZIP63 BY-2 cell line with pSPYCE 35S *Arath*;WEE1. Yellow fluorescence could not be detected. (C) homodimerisation of *Arath*;GF14 ω , transient *Agrobacterium*-mediated transformation of the pSPYNE 35S *Arath*;GF14 ω BY-2 cell line with pSPYCE 35S *Arath*;GF14 ω . Yellow fluorescence was also detected in the nucleus and a small mid section of the cell wall formed between adjacent cells. YFP images were detected at an approximate frequency of 1:6000 Bar scale = 50 μ m.

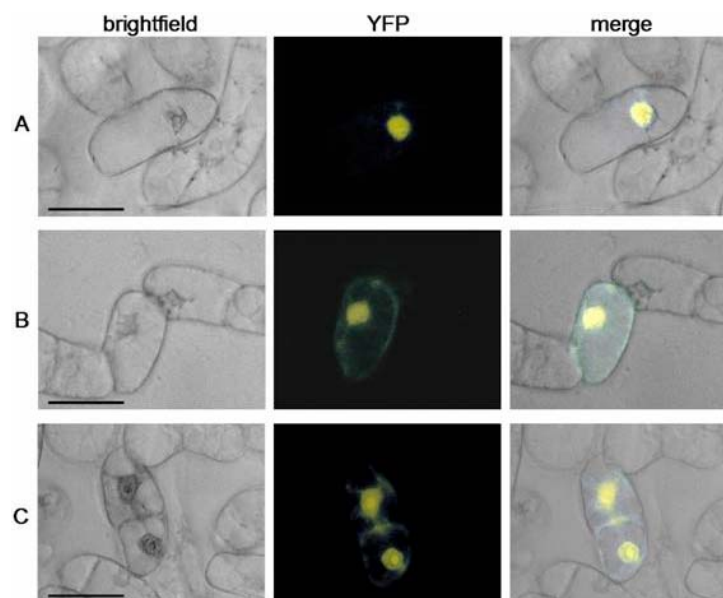


Fig. (4). Cytoplasmic and nuclear Interaction between WEE1 and GF14 ω *in vivo*. BiFC analysis of the *Arath*;WEE1/*Arath*;GF14 ω interaction by transient *Agrobacterium*-mediated transformation of the pSPYNE 35S *Arath*;GF14 ω BY-2 cell line with pSPYCE 35S *Arath*;WEE1. Yellow fluorescence could be detected (A) in the nucleus (B), cell wall of interphase cells and (C) in peripheral cytoplasm and in the wall between two cells. Note that the length of cells in 4C are approximately half that of the labelled cell in 4A suggesting that the former were recently divided. YFP images were detected at an approximate frequency of 1 in 6000. Bar scale = 50 μ m.

Mutation of the *Arath*;WEE1 14-3-3 Binding Site Perturbs Interaction Between *Arath*;WEE1 and *Arath*;GF14 ω

Using motif scanning software (http://scansite.mit.edu/motifscan_seq.phtml), five putative mode I (RSXpSXP) 14-3-3 binding motifs were identified in the protein sequence of *Arath*;WEE1 (Fig. 6A) allowing for low stringency matching. The putative 14-3-3 binding site located at S485 in the C-terminal of *Arath*;WEE1, displays high similarity to the 14-3-3 binding sites located at S549/S558 in mouse and human WEE1, respectively but less so to the corresponding S559 site in *Xenopus* (Fig. 6B). Therefore, S485 in the C-terminal of *Arath*;WEE1 was considered to be the most likely binding site for *Arath*;GF14 ω . An *Arath*;wee1 (S485A) mutant was constructed by site-directed mutagenesis and Y2H used to test whether the abolition of this site in *Arath*;WEE1 affected the interaction with *Arath*;GF14 ω . Growth was not observed when the *wee1*(S485A)/*Arath*;GF14 ω transformant was grown on medium deficient in histidine indicating that the S485A mutation of *Arath*;WEE1 does indeed abolish *Arath*;GF14 ω binding. This was confirmed by a *LacZ* reporter gene filter lift assay and a quantitative liquid ONPG assay (Figs. 7A and B). To test if the interaction was abolished *in vivo*, the tobacco BY-2 cell line carrying pSPYNE 35S *Arath*;GF14 ω was transiently transformed with pSPYCE 35S *Arath*;WEE1 (S485A). Fluorescence was still detected in the nucleus of interphase cells (Fig. 8) but no longer in the cell wall between cells as judged by a scan of $\geq 6,000$ cells (Fig. 8) suggesting that the *Arath*;WEE1 (S485A) mutation perturbs the binding with *Arath*;GF14 ω by restricting the localization of *Arath*;WEE1 to the nucleus.

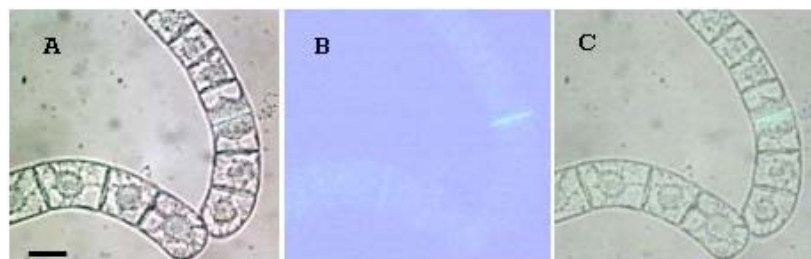


Fig. (5). Cytokinesis. BY-2 cells stained with 0.02% (w/v) aniline blue (A) bright field illumination (B) fluorescence at 420 nm excitation filter (adjusted with auto levels (Adobe Photoshop 6®)) (C) merged image of (A) on greyscale and the primary fluorescent image of (B). Bar scale = 50 μ m.

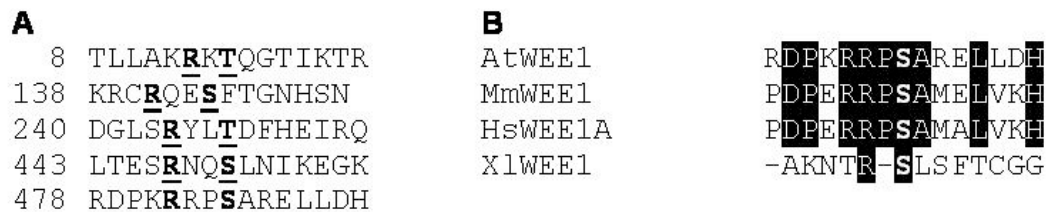


Fig. (6). Mutation of *Arath*;WEE1. (A) The five putative 14-3-3 binding sites identified in the *Arath*;WEE1 protein sequence using a motif scanning software (http://scansite.mit.edu/motifscan_seq.phtml) and the predicted phosphorylation sites (numbers indicate amino acid residue in the *Arath*;WEE1 protein sequence). (B) Line up of the Serine 485 binding site for WEE1 in *Arabidopsis thaliana* (At), with S549 in *Mus musculus* (Mm), S558 in *Homo sapiens* (Hs) and S559 in *Xenopus laevis* (Xl).

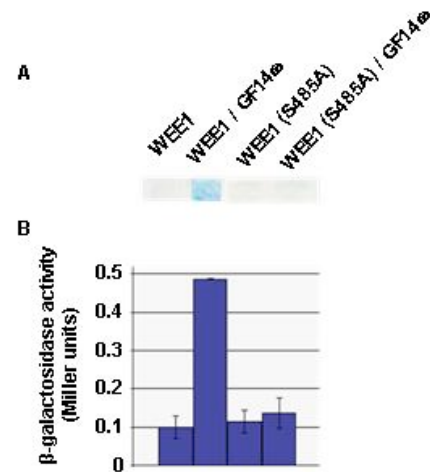


Fig. (7). Mutated WEE1 does not interact with GF14 ω *in vitro*. *LacZ* reporter gene screening: (A) Filter lift assay, from left: *Arath*;WEE1 only, *Arath*;WEE1/*Arath*;GF14 ω , *Arath*;WEE1 (S485A) only and *Arath*;WEE1 (S485A)/*Arath*;GF14 ω . (B) Quantitative ONPG assay, from left *Arath*;WEE1 only, *Arath*;WEE1/*Arath*;GF14 ω , *Arath*;WEE1 (S485A) only and *Arath*;WEE1 (S485A)/*Arath*;GF14 ω (β -galactosidase activity is displayed as mean Miller units \pm SE, n=3).

DISCUSSION

Arath; WEE1/GF14 ω Interaction

A targeted Y2H screen showed that *Arath*;WEE1 interacts with all the *Arabidopsis* Non-Epsilon 14-3-3 isoforms which is consistent with this protein family displaying high sequence conservation (70 – 90%) both at the nucleotide and protein level [44]. Moreover, four of the Non-Epsilon 14-3-3

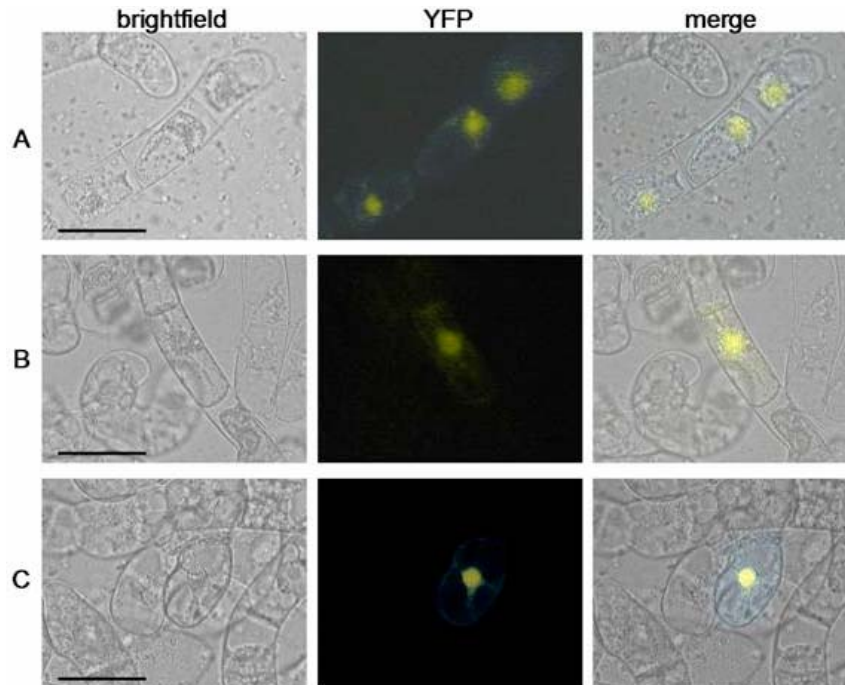


Fig. (8). Mutated WEE1 does not interact with GF14 ω at the cell wall. BiFC analysis of the *Arath*;WEE1 (S485A)/*Arath*;GF14 ω interaction by transient *Agrobacterium*-mediated transformation of the pSPYNE 35S *Arath*;GF14 ω BY-2 cell line with pSPYCE 35S *Arath*;WEE1 (S485A). After 72 h yellow fluorescence could only be detected in the nuclei (A, B and C). YFP images were detected at an approximate frequency of 1:6000. Bar scale = 50 μ m.

proteins tested here (GF14 ϕ , χ , ν and ω) could rescue the *rad24* checkpoint mutant of *S. pombe* [28]. The work then focussed on the Non-Epsilon GF14 ω because like *Arath*;WEE1 [7], it is relatively more highly expressed at the transcript level in proliferative regions of Arabidopsis plants [29] including young roots (data not shown), although unlike *Arath*;WEE1 it is not cell-cycle regulated [38], (and data from Atgene Express).

The specificity of the interaction between *Arath*;WEE1 and *Arath*;GF14 ω was confirmed *in vitro* by co-immunoprecipitation of recombinant proteins. Five mode I 14-3-3 protein binding sites were identified within the *Arath*;WEE1 protein sequence of which one, at S485, showed high similarity to 14-3-3 binding sites reported for other eukaryotes [19-21]. The *arath*;wee1 (S485A) mutant protein was incapable of interacting with *Arath*;GF14 ω in a Y2H screen, suggesting strongly that S485 is the binding site for *Arath*;GF14 ω . A quantitative ONPG assay was performed, which further indicated that the interaction was indeed abolished by the S485A mutation.

Spatial Sub-cellular Localisation

BiFC, besides confirming the *Arath*;WEE1/GF14 ω interaction, indicated that the interaction was located predominantly in the nucleus of interphase cells but additionally in cytoplasmic strands and, we suggest, the wall that forms at cytokinesis. Moreover the frequency of aniline blue-stained cross walls at cytokinesis and BiFC positive cells suggest that the interaction may be at the cell plate. This suggested distribution would be similar to previous work in *Arabidopsis* hypocotyls where a GF14 ω C-terminal:GFP fusion localised to the nucleus, phragmoplast and cytoplasmic periphery

of cells undergoing cytokinesis [39]. However, whilst our localisation of *Arath*;WEE1/GF14 ω for interphase cells was nuclear, most of their GF14 ω ::GFP localisations in interphase cells were cytoplasmic. This differential localisation of GF14 ω may well be because BY-2 interphase cells are predominantly proliferative whereas in *Arabidopsis* hypocotyls, interphase cells are mostly differentiated. GF14 ω ::GFP subcellular localisation in *Arabidopsis* trichomes and guard cells indicated a uniform distribution in the nucleus as well as a spread to components of the cytoskeleton throughout the cytoplasm and cell wall [40] providing a closer match to the GF14 ω homodimer localisation reported here although our cell wall localisations are much weaker than theirs.

When the *arath*;wee1 (S485A) mutant protein was tested against GF14 ω , yellow fluorescence was restricted to the nucleus; it was not detected either in walls between cells or the cytoplasmic periphery of the cell. This suggests that the S485A mutation in the *Arath*;WEE1 affects the binding in plant cells such that the interaction with *Arath*;GF14 ω can no longer occur outside of the nucleus. However the interaction was not completely abolished as might have been expected from the Y2H results. This suggests that the interaction in plant cells may be more complex. When all phosphorylation sites within the three 14-3-3 binding motifs of *S. pombe* Cdc25 were mutated, this reduced the affinity of the binding between 14-3-3 and Cdc25 but did not abolish it [22]. Thus the interaction between *Arath*;GF14 ω and *arath*;wee1 (S485A) may likewise be reduced in affinity and only partially abolished due to the presence of other factors such as other interacting proteins. The BiFC fluorescence cannot be treated as quantitative and hence, a reduction in affinity of the interaction throughout the cell cannot be

excluded. In *Xenopus*, 14-3-3 ϵ binding keeps WEE1 evenly distributed in the nucleus during interphase [20] and is a nuclear protectant from mitogenic cdk-like activity [15]. In human mitotic cells, WEE1 is similarly sequestered in the cytoplasm when an AKT/protein kinase B, phosphorylates WEE1 creating a binding site for 14-3-3 θ [41]. Our observations support a distinctive and differential subcellular distribution of GF14 ω when bound to its client, Arath;WEE1.

HsWEE1 started to re-associate with the nucleus at telophase and in particular was located on the cleavage furrow during cytokinesis [9]. At that time, the authors commented on a cytoplasmic localisation of WEE1 with unknown cytoplasmic factors which might well have been a tethering to a 14-3-3-protein. Arath;WEE1/GF14 ω localisation to the cell plate would fit well with these observations and is intriguing because Arath;WEE1 scored multiple hits with Arath;CDC48A, in a Y2H assay (A. Lentz Grønlund, unpublished data), a protein known to be involved in vesicle formation during plant cytokinesis [42].

In conclusion, our data are consistent with an interaction between Arath;WEE1 and Arath;GF14 ω both *in vitro* and *in vivo*. However, binding between WEE1 and GF14 in the cytoplasm is likely to be the key interaction and would fit with a requirement to disperse WEE1 into the cytoplasm prior to the onset of mitosis.

ACKNOWLEDGEMENTS

We thank Cardiff University, University of Worcester and BBSRC for funding this work and Dr J Kudla (Münster Univ., GE) for kindly supplying us with the BiFC vectors.

REFERENCES

- Morgan DO. Cyclin-dependent kinases: engines, clocks, and microprocessors. *Annu Rev Cell Dev Biol* 2007; 13: 61-91.
- Norbury C, Nurse P. Animal cell cycles and their control. *Annu Rev Biochem* 1992; 61: 41-70.
- O'Farrell PH. Triggering the all-or-nothing switch into mitosis. *Trends Cell Biol* 2001; 11: 12-19.
- Russell P, Nurse P. Negative regulation of mitosis by wee1+, a gene encoding a protein kinase homolog. *Cell* 1987; 49: 59-67.
- McGowan CH, Russell P. Cell cycle regulation of human WEE1. *EMBO J* 1995; 14: 66-75.
- Sun Y, Dilkes BP, Zhang C, *et al.* Characterization of maize (*Zea mays* L.) Wee1 and its activity in developing endosperm. *Proc Natl Acad Sci USA* 1999; 96: 80-85.
- Sorrell DA, Marchbank A, McMahon K, Dickinson JR, Rogers HJ, Francis D. A WEE1 homologue from *Arabidopsis thaliana*. *Planta* 2002; 215: 18-22.
- Gonzalez N, Hernould M, Delmas F, *et al.* Molecular characterization of a WEE1 gene homologue in tomato (*Lycopersicon esculentum* Mill.). *Plant Mol Biol* 2004; 56: 49-61.
- Baldin V, Ducommun B. Subcellular localisation of human wee1 kinase is regulated during the cell cycle. *J Cell Sci* 1995; 108: 25-32.
- Elledge SJ. Cell cycle checkpoints: preventing an identity crisis. *Science* 1996; 274: 64-72.
- Weinert T. DNA damage checkpoints update: getting molecular. *Curr Opin Genet Dev* 1998; 8: 85-93.
- Abraham J, Kelly J, Thibault P, Benchimol S. Post-translational modification of p53 protein in response to ionizing radiation analyzed by mass spectrometry. *J Mol Biol* 2000; 295: 53-64.
- Branzei D, Foiani M. Regulation of DNA repair throughout the cell cycle. *Nat Rev Mol Cell Biol* 2008; 9: 97-08.
- Rhind N, Russell P, Chk1 and Cds1: linchpins of the DNA damage and replication checkpoint pathways. *J Cell Sci* 2000; 113: 89-96.
- Perry JA, Kornbluth S. Cdc25 and Wee1: antagonistic opposites. *Cell Div* 2007; doi:10.1186/1747-1028-2-2.
- Forbes KC, Humphrey T, Enoch T. Suppressors of cdc25p over-expression identify two pathways that influence the G2/M checkpoint in fission yeast. *Genetics* 1998; 150: 61-75.
- Kumagai A, Dunphy WG. Binding of 14-3-3 proteins and nuclear export control the intracellular localization of the mitotic inducer Cdc25. *Genes Dev* 1999; 13: 67-72.
- Yang J, Winkler K, Yoshida M, Kornbluth S. Maintenance of G2 arrest in the *Xenopus* oocyte: a role for 14-3-3-mediated inhibition of Cdc25 nuclear import. *EMBO J* 1999; 18: 74-83.
- Wang Y, Jacobs C, Hook KE, Duan H, Booher RN, Sun Y. Binding of 14-3-3beta to the carboxyl terminus of Wee1 increases Wee1 stability, kinase activity, and G2-M cell population. *Cell Growth Differ* 2000; 11: 11-19.
- Lee J, Kumagai A, Dunphy WG. Positive regulation of Wee1 by Chk1 and 14-3-3 proteins. *Mol Biol Cell* 2001; 12: 51-63.
- Rothblum-Oviatt CJ, Ryan CE, Piwnica-Worms H. 14-3-3 binding regulates catalytic activity of human Wee1 kinase. *Cell Growth Differ* 2001; 12: 81-89.
- Zeng Y, Piwnica-Worms H. DNA damage and replication checkpoints in fission yeast require nuclear exclusion of the Cdc25 phosphatase via 14-3-3 binding. *Mol Cell Biol* 1999; 19: 10-19.
- Graves PR, Lovly CM, Uy GL, Piwnica-Worms H. Localization of human Cdc25C is regulated both by nuclear export and 14-3-3 protein binding. *Oncogene* 2001; 20: 39-51.
- Yaffe MB, Rittinger K, Volinia S, *et al.* The structural basis for 14-3-3-phosphopeptide binding specificity. *Cell* 1997; 91: 61-71.
- Rittinger K, Budman J, Xu J, *et al.* Structural analysis of 14-3-3 phosphopeptide complexes identifies a dual role for the nuclear export signal of 14-3-3 in ligand binding. *Mol Cell* 1999; 4: 53-66.
- DeLille JM, Sehnke PC, Ferl RJ. The Arabidopsis 14-3-3 family of signaling regulators. *Plant Physiol* 2001; 126: 35-8.
- Rosenquist M, Sehnke P, Ferl RJ, Sommarin M, Larsson C. Evolution of the 14-3-3 protein family: does the large number of isoforms in multicellular organisms reflect functional specificity? *J Mol Evol* 2000; 51: 46-58.
- Kuromori T, Yamamoto M. Members of the Arabidopsis 14-3-3 gene family trans-complement two types of defects in fission yeast. *Plant Sci* 2000; 158: 55-61.
- Sorrell DA, Marchbank AM, Chrimes DA, *et al.* The Arabidopsis 14-3-3 protein, GF14omega, binds to the Schizosaccharomyces pombe Cdc25 phosphatase and rescues checkpoint defects in the rad24- mutant. *Planta* 2003; 218: 50-57.
- De Schutter K, Joubes J, Cools T, *et al.* Arabidopsis WEE1 kinase controls cell cycle arrest in response to activation of the DNA integrity checkpoint. *Plant Cell* 2007; 19: 11-25.
- Walter M, Chaban C, Schutze K, *et al.* Visualization of protein interactions in living plant cells using bimolecular fluorescence complementation. *Plant J* 2004; 40: 28-38.
- Bhat RA, Lahaye T, Panstruga R. The visible touch: in planta visualization of protein-protein interactions by fluorophore-based methods. *Plant Methods* 2006; 2: 12.
- Ohad N, Shichrur K, Yalovsky S. The analysis of protein-protein interactions in plants by bimolecular fluorescence complementation. *Plant Physiol* 2007; 145: 90-99.
- Muslin AJ, Tanner JW, Allen PM, Shaw AS. Interaction of 14-3-3 with signaling proteins is mediated by the recognition of phosphoserine. *Cell* 1996; 84: 89-97.
- Muslin AJ, Xing H. 14-3-3 proteins: regulation of subcellular localization by molecular interference. *Cell Signal* 2000; 12: 3-9.
- Chaudhri M, Scarabel M, Aitken A. Mammalian and yeast 14-3-3 isoforms form distinct patterns of dimers *in vivo*. *Biochem Biophys Res Commun* 2003; 300: 79-85.
- Buschmann H, Chan J, Sanchez-Pulido L, Andrade-Navarro MA, Doonan JH, Lloyd CW. Microtubule associated AIR-9 recognizes the cortical division site at pre-prophase and cell plate insertion. *Curr Bio* 2006; 16: 38-43.
- Menges M, De Jager SM, Gruissem W, Murray JAH. Global analysis of the core cell cycle regulators of Arabidopsis identifies novel genes, reveals multiple and highly specific profiles of expression and provides a coherent model for plant cell cycle control. *Plant J* 2005; 41: 46-66.
- Cutler SR, Ehrhardt DW, Griffiths JS, Somerville CR. Random GFP::cDNA fusions enable visualization of subcellular structures in cells of Arabidopsis at a high frequency. *Proc Natl Acad Sci USA* 2000; 97: 18-23.

- [40] Paul A-L, Sehnke PC, Ferl RJ. Isoform-specific subcellular localisation among 14-3-3 proteins in Arabidopsis seems to be driven by client interactions. *Mol Biol Cell* 2005; 16: 35-43.
- [41] Katayama K, Fujita N, Tsuruo T. Aky/protein kinase B-dependent phosphorylation and inactivation of WEE1Hu promote cell cycle progression at G2/M. *Mol Cell Biol* 2005; 25: 25-37.
- [42] Rancour DM, Dickey CE, Park S, Bednarek SY. Characterization of AtCDC48. Evidence for multiple membrane fusion mechanisms at the plane of cell division in plants. *Plant Physiol* 2002; 130: 41-53.
- [43] An GH. High efficiency transformation of cultured tobacco cells. *Plant Physiol* 1985; 79: 568-70.
- [44] Wu K, Rooney MF, Ferl RJ. The Arabidopsis 14-3-3 multigene family. *Plant Physiol* 1997; 114: 1421-31.

Received: March 3, 2009

Revised: April 20, 2009

Accepted: May 21, 2009

© Grønlund *et al.*; Licensee *Bentham Open*.

This is an open access article licensed under the terms of the Creative Commons Attribution Non-Commercial License (<http://creativecommons.org/licenses/by-nc/3.0/>) which permits unrestricted, non-commercial use, distribution and reproduction in any medium, provided the work is properly cited.